



## Research article

# Bulk and single-cell sequencing identified a prognostic model based on the macrophage and lipid metabolism related signatures for osteosarcoma patients

Zili Lin<sup>a</sup>, Ziyi Wu<sup>c</sup>, Wei Luo<sup>a,b,\*</sup><sup>a</sup> Department of Orthopaedics, Xiangya Hospital, Central South University, Changsha, Hunan, 410008, PR China<sup>b</sup> National Clinical Research Center for Geriatric Disorders, Xiangya Hospital, Changsha, Hunan, 410008, PR China<sup>c</sup> Department of Orthopaedics, the Second Xiangya Hospital, Central South University, Changsha, Hunan, 410011, PR China

## ARTICLE INFO

## Keywords:

Osteosarcoma  
Macrophage  
Lipid metabolism  
Chemoresistance  
Immune infiltration

## ABSTRACT

The introduction of multidrug combination chemotherapy has significantly advanced the long-term survival prospects for osteosarcoma (OS) patients over the past decades. However, the escalating prevalence of chemoresistance has emerged as a substantial impediment to further advancements, necessitating the formulation of innovative strategies. Our present study leveraged sophisticated bulk and single-cell sequencing techniques to scrutinize the OS immune microenvironment, unveiling a potential association between the differentiation state of macrophages and the efficacy of OS chemotherapy. Notably, we observed that a heightened presence of lipid metabolism genes and pathways in predifferentiated macrophages, constituting the major cluster of OS patients exhibiting a less favorable response to chemotherapy. Subsequently, we developed a robust Macrophage and Lipid Metabolism (MLMR) risk model and a nomogram, both of which demonstrated commendable prognostic predictive performance. Furthermore, a comprehensive investigation into the underlying mechanisms of the risk model revealed intricate associations with variations in the immune response among OS patients. Finally, our meticulous drug sensitivity analysis identified a spectrum of potential therapeutic agents for OS, including AZD2014, Sunitinib, Buparlisib, Afuresertib, MIRA-1, and BIBR-1532. These findings significantly augment the therapeutic arsenal available to clinicians managing OS, presenting a promising avenue for elevating treatment outcomes.

## 1. Introduction

Osteosarcoma (OS), recognized as the most prevalent primary bone malignancy, is characterized by intratumoral osteogenesis and displays a high incidence rate among adolescents [1,2]. To date, the implementation of standardized treatments, which encompass surgical intervention, chemotherapy, and neoadjuvant chemotherapy, has notably augmented the long-term survival rates of patients diagnosed with localized osteosarcoma [2]. Regrettably, therapeutic outcomes and prognoses for patients confronting unresectable, recurrent, and metastatic OS remain dauntingly bleak, with a meager 5-year survival rate hovering around 20% [3,4]. Furthermore, the escalating emergence of chemoresistance poses a substantial impediment to the advancement of therapeutic strategies for patients with localized primary OS, as their 5-year survival rate plateaus at approximately 60–70% [5]. Previous investigations have

\* Corresponding author. Department of Orthopaedics, Xiangya Hospital, Central South University, Changsha, Hunan 410008, PR China.  
E-mail address: [luoweixy@csu.edu.cn](mailto:luoweixy@csu.edu.cn) (W. Luo).

<https://doi.org/10.1016/j.heliyon.2024.e26091>

Received 17 November 2023; Received in revised form 7 February 2024; Accepted 7 February 2024

Available online 18 February 2024

2405-8440/Â© 2024 Published by Elsevier Ltd. This is an open access article under the CC BY-NC-ND license (<http://creativecommons.org/licenses/by-nc-nd/4.0/>).

underscored OS as one of the most heterogeneous tumors, contributing to its suboptimal responses to chemotherapy and targeted therapies [3,6]. The genetic complexity and instability of OS cells present an exceedingly formidable challenge for precisely targeting OS cells [7], necessitating the exploration of new research directions.

In recent decades, immunotherapies have revolutionized cancer research and treatment, demonstrating enduring clinical responses in specific malignancies [8–12]. The immune system provides humans with immunosurveillance, including the adaptive and innate immune systems, to eliminate constantly emerging cancer cells, protecting humans from malignancy [13]. Conversely, the compromise or elimination of the immune system can lead to unbridled tumor cell proliferation and substantial progression [13]. Paradoxically, essential components of the human body's defense, such as macrophages, can be coopted by cancer cells, transforming them into steadfast allies that resist external treatments [13,14]. Investigating the mechanisms through which cancer cells manipulate these immune guardians represents a promising avenue for therapeutic exploration [14]. Macrophages, recognized for their phagocytic, antigen-presenting, and immune-regulating capabilities, serve as a critical nexus between innate and adaptive immunity [15]. Responding to microenvironmental cues, macrophages polarize into inflammation-promoting M1 and anti-inflammatory M2 clusters, corresponding to cancer-promoting M1 and anticancer M2 macrophages [15]. Prevailing research suggests that heightened macrophage infiltration correlates with a poor prognosis in cancer patients [16,17]. Conversely, a prior study indicated that elevated expression of macrophage-related genes and increased macrophage infiltration in OS tissue were associated with metastasis suppression [18]. However, other investigations illuminated the tumor-promoting role of tumor-associated macrophages (TAMs), particularly M2 macrophages, facilitating tumor invasive capabilities through inflammation or angiogenesis [19–21]. Targeting M2 polarization has exhibited anti-metastatic efficacy and the attenuation of stem cell-like properties in OS [22–24]. Consequently, the impact of macrophages on OS appears contingent upon their metabolic and polarized state.

Lipid metabolism dysregulation has been observed in various cancers that exploits lipid metabolism for energy requirement, cellular component, and various signaling pathways including cell proliferation, apoptosis, metastasis, drug-resistance, and interaction with the tumor microenvironment [25–27]. Lipid metabolism orchestrate immune cell responses and manipulating lipid metabolism may restructure the interaction among cancer cells, immune cells, and stromal to exert a tumor-promoting or anti-tumor effect [28–30]. Mounting evidence has proved that lipid metabolism can regulate macrophage functions through influencing signal transduction and gene expression [30,31]. In most situation, TAMs upregulate the expression of CD36, the scavenger receptor, to accumulate lipid, triggering metabolism transformation from glycolysis to fatty acid oxidation [30,32,33]. Subsequently, these metabolism changes will result in a series of intracellular reactions such as the enhancement of oxidative phosphorylation, elevated reactive oxygen species, and phosphorylation of JAK1, leading to the anomalous transcriptional activity and eventually regulating TAMs generation and function [30,32,34]. Therefore, targeting TAMs lipid metabolism may serve as a potential therapeutic method for cancer treatments.

Herein, through a comprehensive approach encompassing both single-cell and bulk transcriptome analyses, we have identified a potential association between the metabolic transformation of macrophages and the therapeutic effects of OS chemotherapy. This underscores the prospect that targeting the metabolism of macrophages could represent a promising therapeutic avenue for individuals with OS. Finally, we have developed a model that integrates macrophage and lipid metabolism-related factors to predict prognosis, delineate the immune landscape, and ascertain drug sensitivity in OS patients, offering new insights into potential strategies for enhancing OS treatments.

## 2. Materials and methods

### 2.1. Data acquisition and processing

The RNA sequencing data and clinical information of 85 OS patients in TARGET-OS cohort were downloaded from UCSC Xena (<https://xena.ucsc.edu>) website. Additionally, the RNA sequencing data and the corresponding clinical information of 50 OS patients in GSE21257 dataset, 50 OS samples in GSE154540 dataset and 9 single-cell sequencing samples in GSE152048 dataset were downloaded from the Gene Expression Omnibus (GEO) database (<https://www.ncbi.nlm.nih.gov/geo>). The 187 metabolic-related pathways and the corresponding genes and 1399 lipid metabolism related genes (LMRGs) of the gene set GOBP\_LIPID\_METABOLIC\_PROCESS were acquired from the Molecular Signatures Database (MSigDB: <https://www.gsea-msigdb.org/gsea/msigdb>). For bulk transcriptome data, background correction and normalization were performed for the gene expression matrix of GEO and Xena website and R package "inSilicoMerging" and "sva" were utilized to merge and remove the batch effects for TARGET-OS and GSE21257 datasets [35,36]. For single-cell transcriptome data, "Seurat" package was utilized for quality control, normalization, hypervariable genes selection, dimensionality reduction, and clustering after the dataset merging and de batching of "Harmony" package [37,38]. In line with the policies and guidelines of the Xena and GEO databases, these data were utilized for our researches.

### 2.2. Unsupervised clustering of metabolic-related pathways

ConsensusClusterPlus was utilized to perform cluster analysis, using agglomerative kmdist clustering with a 1-pearson correlation distances and resampling 80% of the samples for 10 repetitions [39]. The optimal number of clusters was determined using the empirical cumulative distribution function plot. Subsequently, "PCA" plot and Kaplan-Meier plot were utilized to verified the resolving ability of the clustering [40]. Then, differentially expressed analysis was performed for the clusters, and the genes with p value < 0.05 and fold change >2 were identified as the differentially expressed genes (DEGs). Additionally, functional enrichment analyses, including Gene ontology (GO), Kyoto Encyclopedia of Genes and Genomes (KEGG), Gene Set Enrichment Analysis (GSEA), and Gene

Set Variation Analysis (GSVA), were performed for the clusters [41]. Furthermore, Estimation of Stromal and Immune cells in Malignant Tumor tissues using Expression data (ESTIMATE) and Cell type identification by estimating relative subsets of RNA transcripts (CIBERSORT) analyses were performed to assess the immune landscape of OS patients [42,43].

### 2.3. Exploration of OS single-cell data

R package "CommPath" was utilized to exhibit the intercellular communication chain among different cell clusters [44]. "SCORPIUS" package was employed to display the developmental trajectory of macrophages [45]. The metabolic activation fraction of macrophages were explored using "scMetabolism" package [46].

### 2.4. Weighted gene Co-expression network analysis (WGCNA)

The genes with the top 3000 mad in the expression matrix of TARGET-OS data were selected to construct WGCNA network, with R square = 0.9 being cut-off value of the soft threshold [47]. After the construction of WGCNA, the relationship between the modules and macrophages were explored and the macrophage-related genes were identified for the subsequent analyses.

### 2.5. Construction and validation of the prognostic model

Venn plot was employed to identified the intersected genes between macrophage-related genes and lipid metabolism-related genes

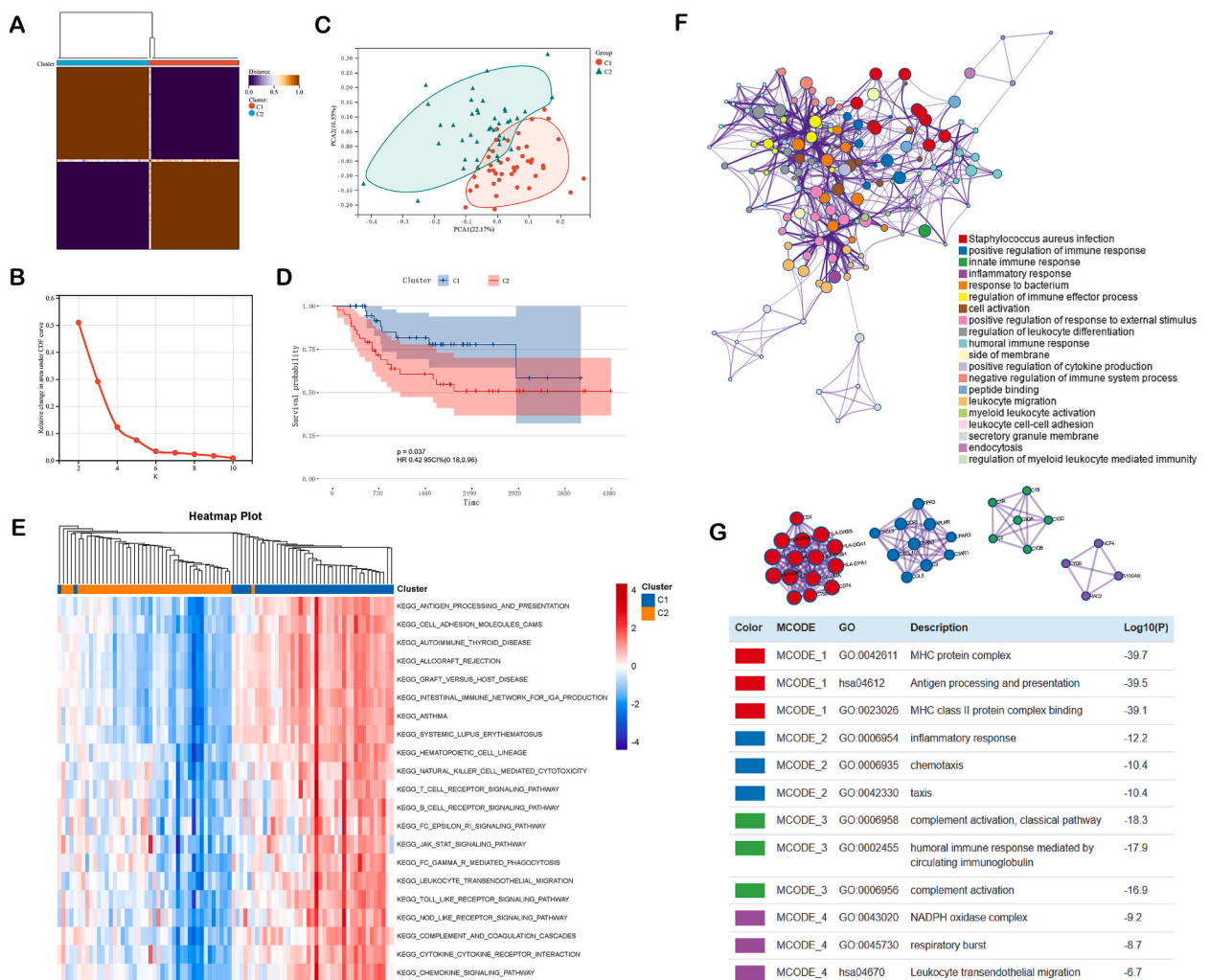


**Fig. 1.** Identification of metabolism-related clusters. (A–C) Two clusters were identified as the optimal option for consensus clustering. (D) Kaplan-Meier plot of two clusters. (E) Metabolic heatmap of two clusters. (F) The functional enrichment analyses of DEGs between two clusters. (G) The functional module of DEGs. DEGs: differentially expressed genes; GSEA: Gene Set Enrichment Analysis.

(called MLMGs). Subsequently, univariate and multivariate Cox regression analyses were introduced to select the prognostic MLMGs for the construction of the prognostic model. The risk model can be expressed as follows: Risk score =  $\sum \text{Coefficient}_{\text{mRNA}_i} * \text{Expression}_{\text{mRNA}_i}$ , in which  $\text{Coefficient}_{\text{mRNA}_i}$  represented the weighting coefficient of the MLMGs and  $\text{Expression}_{\text{mRNA}_i}$  represented the expression levels of the MLMGs. Patients were divided into high- and low-risk groups based on the median risk scores. Then, Kaplan-Meier plot were utilized for the training group TARGET-OS cohort and the testing group GSE21257 cohort, and their merged cohort, with the corresponding receiver operating characteristic (ROC) curve depicted.

2.6. Mechanism exploration of the risk model

DEGs with the same selection standard like above were identified in the merged group and undergone GO and KEGG analyses. Additionally, GSEA was performed for further exploration of functional enrichment and ESTIMATE analysis was employed to evaluate the immune situation between high- and low-risk groups.

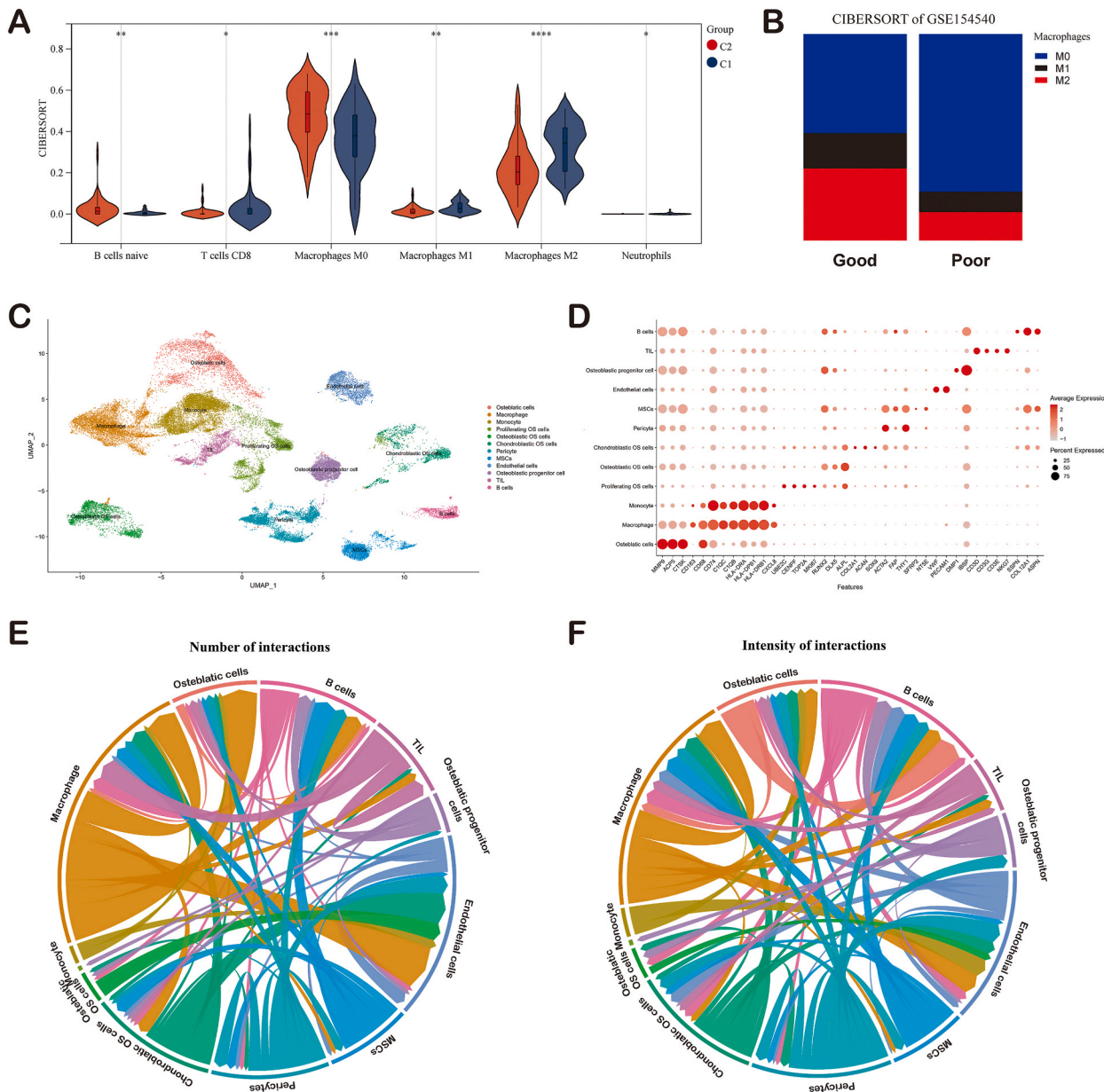


**Fig. 2.** Macrophages plays an important role in OS tumor microenvironment. (A) The CIBERSORT analysis of two clusters. (B) The CIBERSORT analysis of the GSE154540 dataset. (C–D) Cell clustering in the single-cell landscape. (E–F) The number and intensity of cell-cell communication.

2.7. Construction and validation of the MLMR nomogram

The multivariate cox regression analysis was implemented for the risk score and other clinical traits including age, gender, and metastasis, and the factors (p value < 0.05) were included in the integrated nomogram. Subsequently, the calibration curve, timeROC curve, and timeDCA curve of the nomogram were depicted to validate the accuracy and clinical usefulness of the nomogram.

2.8. Potential therapeutic drug screening

Drug sensitivity analysis between high- and low-risk group were performed using the "limma", "ggpubr", and "oncoPredict" packages for the exploration of OS potential therapeutic drugs [48–50].

2.9. Statistical analyses

R software (version 4.2.1) was applied for statistical analyses. Log-rank method was used for the univariate regression analysis and Kaplan-Meier plot. Stepwise regression was performed for the multivariate regression analysis. A P-value < 0.05 was regarded as

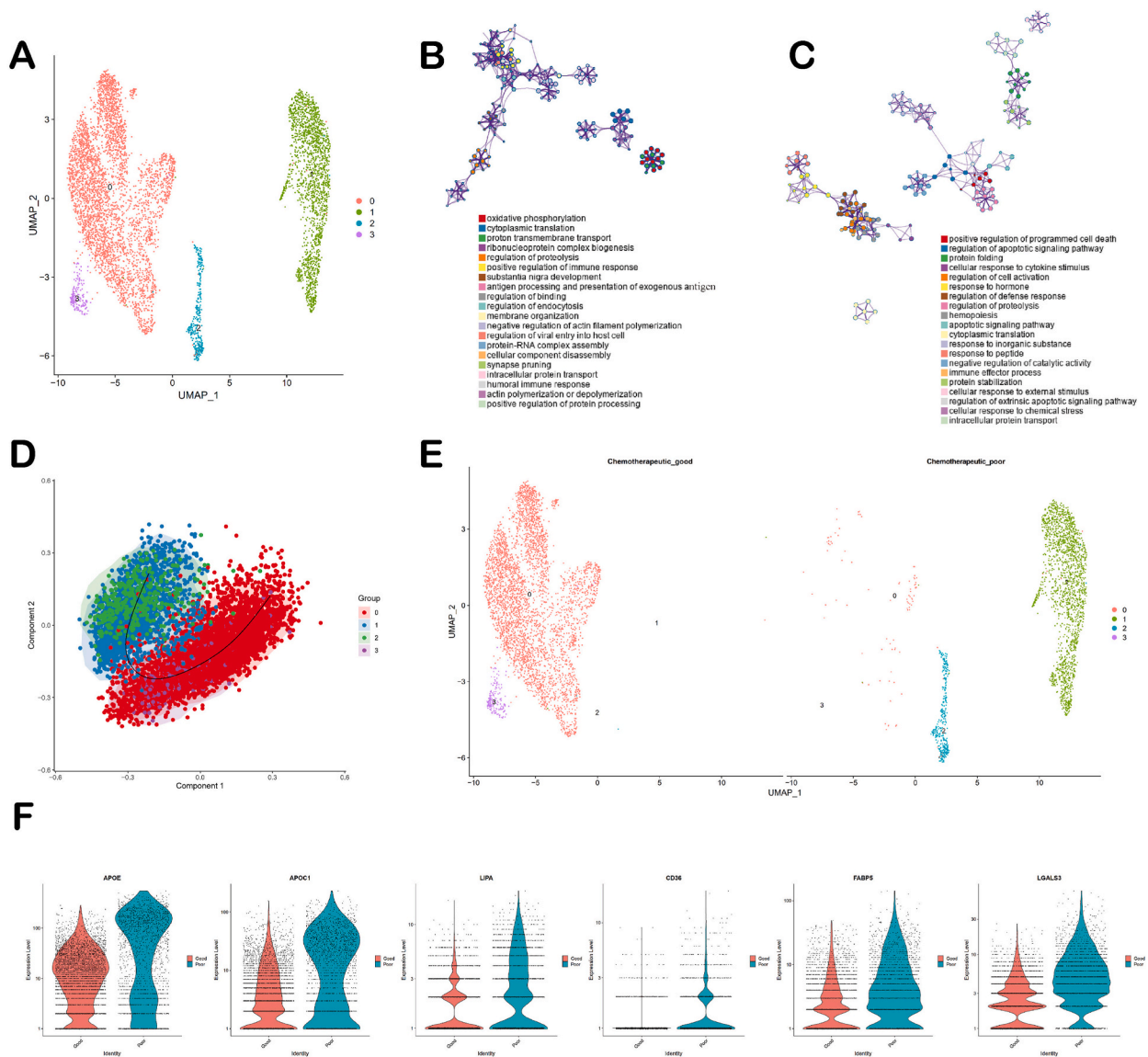


**Fig. 3.** The differentiation status and metabolism of macrophages may be associated with OS chemotherapeutic effect. (A) Clustering of macrophages. (B–C) The functional enrichment analyses of macrophages clusters. (D) The trajectories analysis of macrophages. (E–F) Lipid metabolism genes between the good- and poor-chemotherapeutic groups.

statistically different.

### 3. Results

#### 3.1. Immune situation is associated with the prognosis of OS patients

Accumulated evidence has highlighted the vital role of metabolism in cancer progression. To explore the role of metabolism in OS, unsupervised clustering based on 187 metabolic-related pathways was performed (Table S1). Interestingly, OS patients seem to exhibit certain characteristics and divided into two clusters in term of metabolism-related pathways (Fig. 1 A.B, Fig. S1 A.B). The PCA plot exhibited that these two clusters excellently distinguished each other, with a distinct prognosis detected via Kaplan-Meier plot [ $p = 0.037$ , (HR = 0.42, 95CI%: 0.18–0.96)] (Fig. 1 C.D). Notably, immune-related pathway such as antigen processing and presentation, B cell receptor signaling pathway, and natural killer cell mediated cytotoxicity were significantly enriched in the cluster 1 that exhibited a better prognosis, which suggested that immune situation of OS patient may affect their prognoses (Fig. 1 E). To confirm this assumption, the functional enrichment including GO and KEGG analyses for the DEGs between two clusters were employed, and 140 identified DEGs were most enriched in immune-related pathways, including positive regulation of immune response, innate immune response, regulation of immune effector process and so on (Fig. 1F–Tables S2–3). Additionally, four functional modules constructed by DEGs also focused on MHC protein complex, antigen processing and presentation, inflammatory response, complement activation, which were significantly associated with immune processes (Fig. 1 G). Furthermore, GSEA based on KEGG functional sets and GSEA based on the hallmark gene set further confirmed these results (Fig. 1 C.D). Subsequently, to elaborate the immune landscape between these two clusters, we performed immune infiltration analyses including ESTIMATE and CIBERSORT algorithm. The ESTIMATE algorithm found that compared with cluster 2 that possessed a worse prognosis, cluster 1 significantly exhibited a more excellent stromal score, immune score, and estimate score while displayed a lower tumor purity (Fig. 2 A, Fig. 1 E). Additionally, the CIBERSORT algorithm exhibited that the distributance of B cells naive, T cells CD8, macrophages M0, macrophages M1, macrophages M2, and neutrophils were significantly different between these two clusters. Notably, macrophages were more different, and polarized macrophages were more enriched in cluster 1 while unpolarized macrophages were more found in cluster 2, which may indicate that macrophages with different polarization states may be associated with the progression and prognosis of OS patients (Fig. 2 A). Given that chemotherapeutic effects was one of the most significant prognostic factors for OS patients, we speculated that macrophages with different polarization states may be associated with that chemotherapeutic effects of OS patients. For validating this hypothesis, we performed CIBERSORT algorithm for 50 OS patients in GSE154540 cohort and found that compared with the patients with good chemotherapeutic effects, the patients with poor chemotherapeutic effects exhibited more unpolarized macrophages and less polarized macrophages (Fig. 2 B). Therefore, the polarization states of macrophages may be associated with the chemotherapeutic effects and prognosis of OS patients.

#### 3.2. The differentiation states of macrophages may be associated with the chemotherapeutic effects of OS patients

To further explore the role of macrophages in the chemotherapeutic effects of OS patients, we performed a single-cell level analysis for GSE152048 data set which including both good- and poor-chemotherapeutic OS patients. Based on the biomarkers, we classified cells of OS tissues into 12 clusters: osteoblastic cells, macrophages, monocytes, proliferating OS cells, osteoblastic OS cells, chondroblastic OS cells, perocytes, MSCs, endothelial cells, osteoblastic progenitor cells, TILs, and B cells (Fig. 2 C.D, Fig. 2 A). Then, we performed the intercellular communication analysis to explore the interaction among all cell clusters and discovered that the interaction between macrophages and other cell clusters were abundant and intense, indicating the important role of macrophages among the tumor microenvironment (TME) of OS (Fig. 2 E.F). Subsequently, to further explore the characteristics of macrophages, we extracted macrophages from all cell clusters and clustered them into four clusters (Fig. 3 A). To illuminate the function of macrophage clusters, we performed the functional enrichment for each macrophage cluster based on their marker genes. The top20 GO results of cluster 0 macrophage indicated that this cluster was inclined to metabolically and immunologically active macrophages, which were enriched in the metabolism and immune related pathway, such as oxidative phosphorylation, cytoplasmic translation, positive regulation of immune response, antigen processing and presentation of exogenous antigen. The top20 GO results of cluster 1 macrophage exhibited that this cluster was likely to be apoptosis-regulating macrophages, which were enriched in apoptosis related pathways, such as positive regulation of programmed cell death, regulation of apoptotic signaling pathway, regulation of cell activation, and apoptotic signaling pathway (Fig. 3 B.C). Additionally, macrophages in cluster 2 was a macrophage phenotype intermediate between cluster 0 and cluster 1 while cluster 3 exhibited matrix metabolic phenotype (Fig. 2 C.D). Furthermore, to reveal the developmental trajectory of the macrophage clusters, we performed pseudotemporal dynamics analysis and found that macrophages in cluster 0 and 3 were developed from cluster 1 and 2, which hinted that cluster 1 and 2 may represent naive macrophage phenotype while cluster 0 and 3 exhibited more mature phenotype (Fig. 3D–S 2 B). Interestingly, we found that macrophages of cluster 0 and 3 almost were derived from OS patients with good chemotherapeutic effects while that of cluster 1 and 2 were the main macrophages from OS patients with poor chemotherapeutic effects (Fig. 3 E). Therefore, the differentiation states of macrophages may be associated with the chemotherapeutic effects of OS patients, and the poorly differentiated macrophages may attribute to poor chemotherapy response.

3.3. Lipid metabolism and macrophage related risk model was an excellent prognostic predictor for OS patients

To further explore the functions of macrophages between OS patients with good- and poor-chemotherapeutic effects, we performed a metabolic analysis and found that compared with the good-chemotherapeutic groups, the poor-chemotherapeutic groups exhibited more enrichment of lipid metabolism pathways (Fig. 2 E). Meantime, lipid metabolism biomarkers displayed higher expression in poor-chemotherapeutic groups (Fig. 3 F), which indicated that lipid metabolism may be associated with the functions of macrophages. Subsequently, to excavate the prognostic value of both macrophage and lipid metabolism, we tried to establish a macrophage and lipid metabolism related (MLMR) risk model. In terms of the macrophage related genes, we initially utilized WGCNA to identified the biological functional module and roughly obtained 10 modules (Fig. 4 A). Subsequently, we implemented correlation analyses between these modules and various immune cell types and found that the brown module was highly correlated with macrophages infiltration. The module-trait relationship heatmap indicated that the genes in the brown module were negatively correlated with M0 macrophages filtration but positively correlated with M1 and M2 macrophages infiltration (Fig. 4 B). Then, we intersected 501 genes in the brown module, which called macrophage related genes, with 1399 lipid metabolism genes to gain the MLMRGs and 49 MLMRGs were identified to established the MLMR risk model (Fig. 4 C). Through univariate Cox regression analysis, ten prognostic MLMRGs

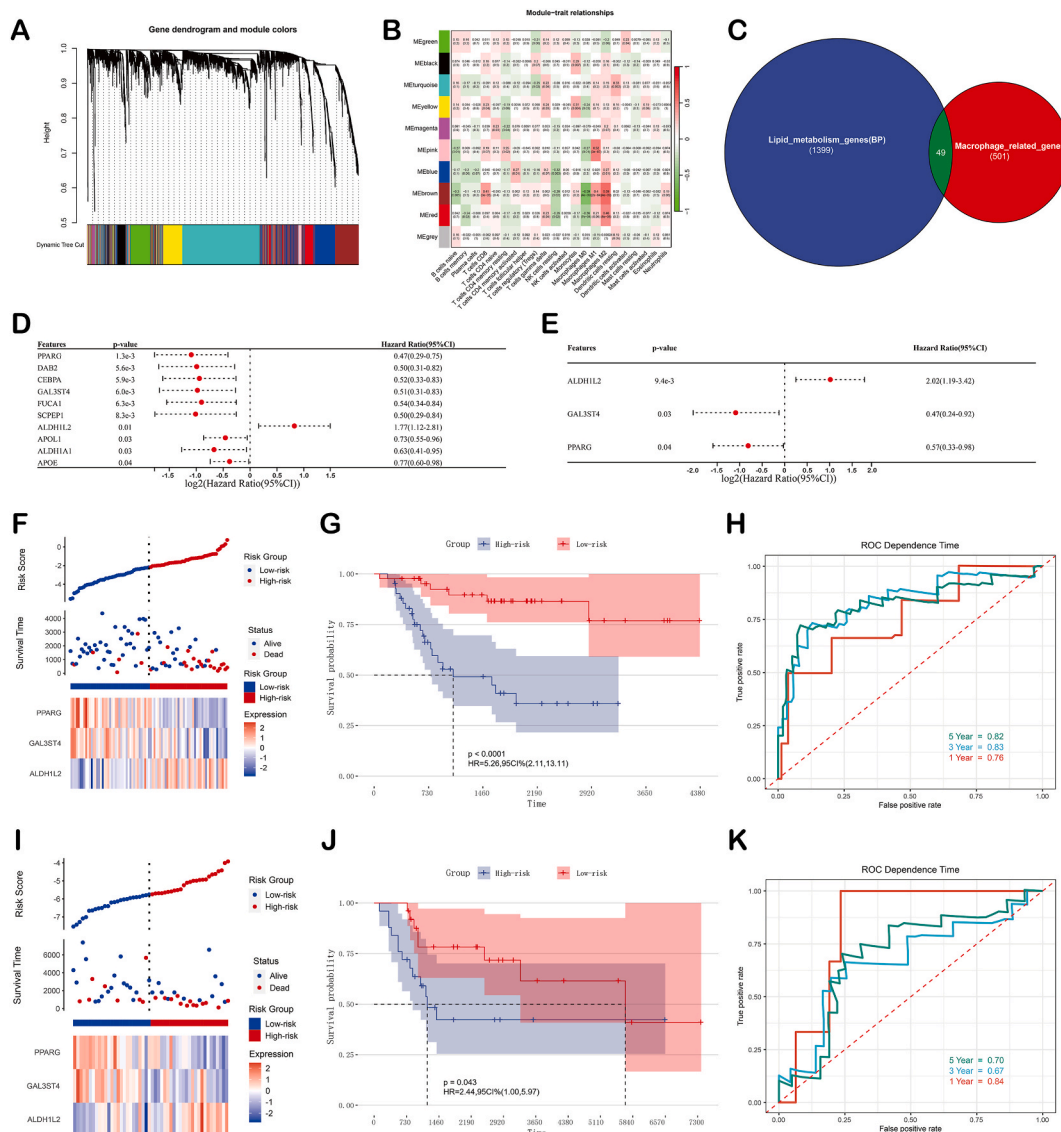


**Fig. 4.** Construction and validation of the prognostic model. (A–C) Identification of MLMRGs. (D–E) Identification of the independent prognostic MLMRGs. (F–H) Distribution, Kaplan-Meier plot, and Time-dependent ROC curve of the risk model in TARGET-OS cohort. (I–K) Distribution, Kaplan-Meier plot, and Time-dependent ROC curve of the risk model in GSE21257 cohort. MLMRGs: Macrophage and lipid metabolism related genes.

were identified and then undergone multivariate Cox regression analysis to eliminate the interaction effect among these gene (Fig. 4 D. E). Finally, a MLMRG risk model was established and expressed as follow: risk score =  $0.70 \times \text{ALDH1L2} - 0.76 \times \text{GAL3ST4} - 0.56 \times \text{PPARG}$ . To validate the prognostic predictive ability of the risk model, we classified OS patients into high- and low-risk group based on the median risk score. As expected, in both the training set and the test set, we found that both the expression of PPARG and GAL3ST4 were higher in the low-risk group while the expression of ALDH1L2 was higher in the high-risk group, which was consistent with the result of the multivariate regression analysis. Meantime, the Kaplan-Meier curve of the training group exhibited an excellent prognostic predictive ability [ p value < 0.0001; HR = 5.26, 95CI%(2.11, 13.11)], with 1-, 3-, and 5-year receiver operating characteristic (ROC) curve being 0.76, 0.83, and 0.82 (Fig. 4F–H). Similarly, the performance of the risk model was also validated in the testing group and a viable prognostic predictive ability was uncovered [ p value = 0.043; HR = 2.44, 95CI%(1.00, 5.97)], with 1-, 3-, and 5-year receiver operating characteristic (ROC) curve being 0.84, 0.67, and 0.70 (Fig. 4I–K). Together, our risk model exhibited an excellent performance in term of the prognostic predictive ability and could be utilized as a potential prognostic predictor for OS patients.

### 3.4. Mechanism exploration of the risk model

The underlying mechanism of the MLMR risk model affected the prognosis of OS patients was further explored. The above two cohorts were merged into a larger cohort and the equally excellent predictive ability was observed in the merged cohort [ p value < 0.0001; HR = 3.33, 95CI%(1.78, 6.25)], with 1-, 3-, and 5-year receiver operating characteristic (ROC) curve being 0.81, 0.76, and 0.76 (Fig. 5 A-C, Fig. 2 F). Then, the DEA was implemented and identified 44 DEGs, in which were mostly enriched in the immune related pathways, such as innate immune response, inflammatory response, inflammatory response, regulation of immune effector process, and immunoglobulin mediated immune response (Fig. 5 D). Meantime, the underlying mechanism was validated by the GSEA analysis, which indicated that immune related pathways, including antigen processing and presentation, cytokine-cytokine receptor interaction, FC

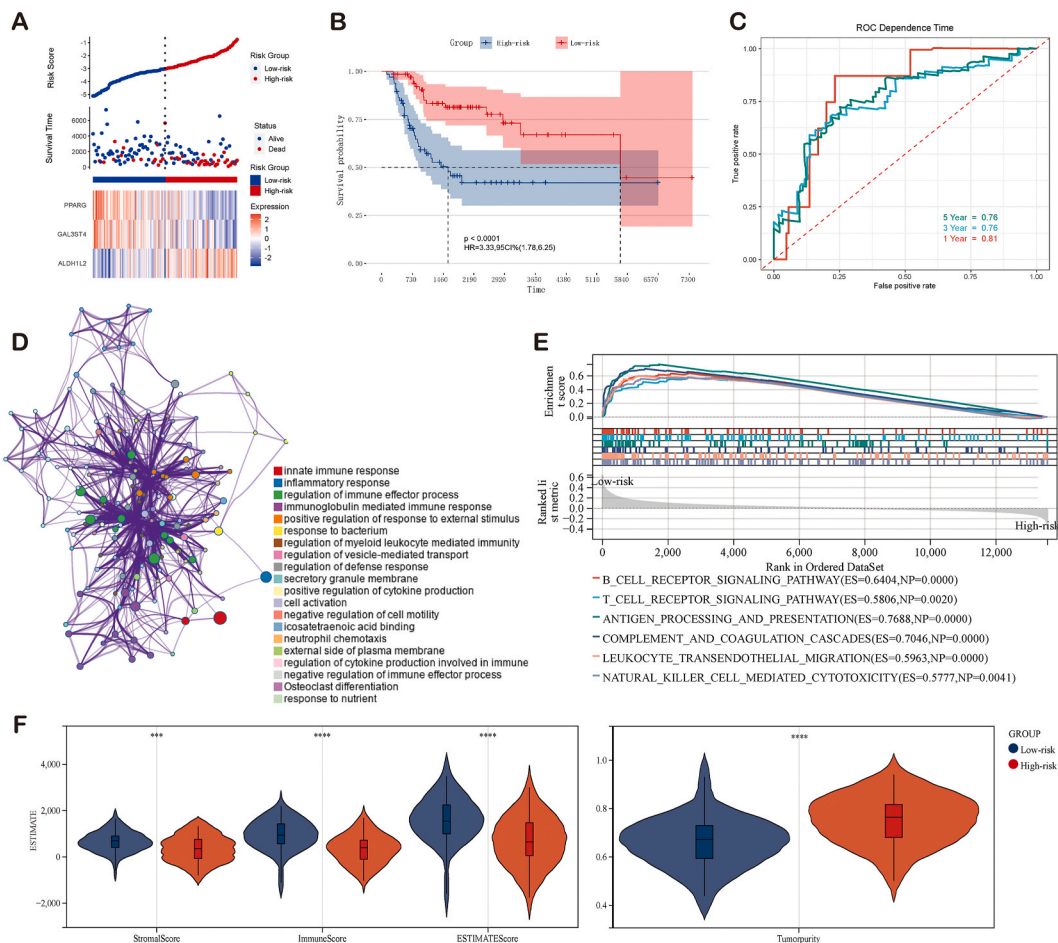


**Fig. 5.** Mechanism exploration of the MLMR risk model. (A–C) Distribution, Kaplan-Meier plot, and Time-dependent ROC curve of the risk model in the merged cohort. (D) The protein-protein interaction network and functional enrichment analysis of DEGs between high- and low-risk groups. (E) The GSEA between high- and low-risk groups. (F) The CIBERSORT analysis of the high- and low-risk groups. DEGs: differentially expressed genes.

GAMMA R mediated phagocytosis, Toll like receptor signaling pathway, B cell receptor signaling pathway, and natural killer cell receptor signaling pathway, were more enriched in the low-risk group (Fig. 5 E). Considering the significant enrichment of the immune related pathways, we tried to investigate the immune infiltration difference between the high- and low-risk groups. As expected, the ESTIMATE algorithm displayed that compared with that of the high-risk group, the stromal score, immune score, and estimate score of the low-risk group were significantly higher while the tumor purity was lower (Fig. 5 F). Collectively, the difference of immune response between the high- and low-risk groups may contribute to their prognostic discrepancy.

3.5. MLMR nomogram exhibited a distinguished performance for the predictive ability of OS patients

To quantitatively predict the survival rate of OS patients and provide more precise treatment, we established a nomogram integrated risk score and clinical prognostic factors. Firstly, multivariate Cox regression analysis was employed for the risk score and the corresponding clinical characteristics, including age, metastasis, primary site, and gender, to identify the independent risk factors for OS patients. As shown in the figure, the metastasis ( $p = 2.8 \times 10^{-8}$ ), risk score ( $p = 9.8 \times 10^{-6}$ ), and primary site ( $p = 1.1 \times 10^{-3}$ ) of OS patients were mostly associated with the prognoses of OS patients (Fig. 6 A). Subsequently, these three factors were included to construct an integrated nomogram, in which each patient could obtain his/her 3- and 5-year survival rate based on the sum of each score derived from his/her metastasis, risk score, and primary site (Fig. 6 B). Then, to validate the performance of the established nomogram, we depicted the corresponding calibration curve, timeROC and timeDCA plots. The calibration curve indicated the excellent 3- and 5-year Goodness of Fit Index (GFI) of the nomogram and the timeROC plot confirmed the corresponding predictive

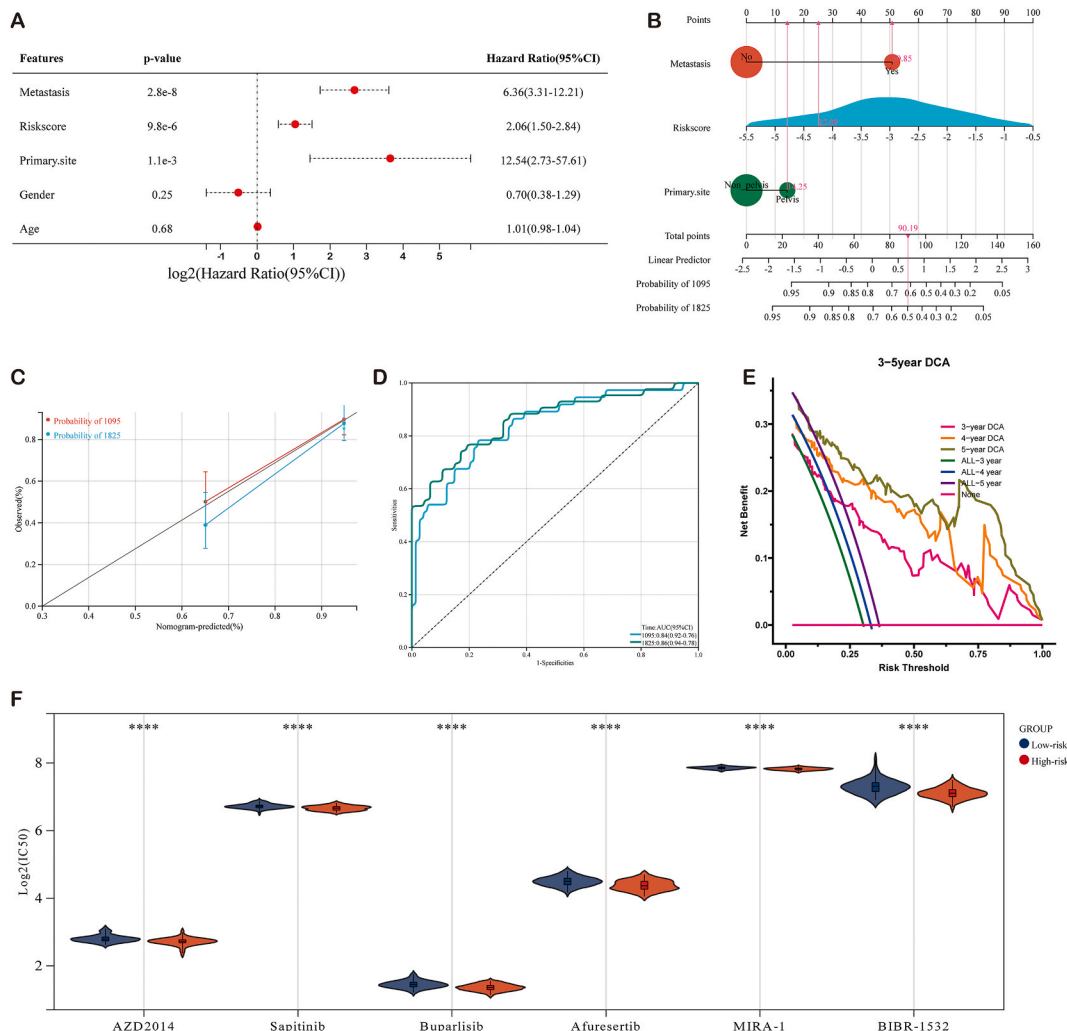


Fig. 6. Construction and validation of the integrated nomogram. (A) The result of multivariate Cox regression of risk score and clinical traits, including metastasis, age, primary site, and gender. (B) The integrated nomogram combines risk score, primary site, and metastasis. (C) The calibration curve of the nomogram. (D) The timeROC curve of the nomogram. (E) The timeDCA curve of the nomogram. (F) Drug sensitivity analysis. ROC: Receiver Operating Characteristic; DCA: decision curve analysis.

accuracy [3-year: 0.84 (0.76–0.92), 5-year: 0.86 (0.78–0.94)] (Fig. 6 C,D). Furthermore, the timeDCA plot displayed that the established nomogram possessed the outstanding clinical usefulness (Fig. 6 E). Collectively, our integrated nomogram may provide more precise prognostic information for the clinicians, optimizing OS treatment.

### 3.6. Screening of potential therapeutic drugs

Increasing chemoresistance has challenged the therapeutic improvement of OS patients, implying the urgency to exploit OS potential drugs. Through the exploration of GDSC database, we identified a series of OS potential drugs and the six most potential drugs were AZD2014, Sapitinib, Buparlisib, Afuresertib, MIRA-1, and BIBR-1532 (Fig. 6 F). All of these six drugs possessed a lower IC50 in the high-risk group, indicating these drugs may be effective for the refractory OS.

## 4. Discussion

The integration of multidisciplinary therapeutic approaches has significantly augmented the long-term survival rates of OS patients [2]. However, the escalating challenge of chemoresistance remains a formidable obstacle, impeding the continuous progress of OS treatments over the decades [7]. The intrinsic complexity and genomic instability of OS underscore the pressing need for a profound comprehension of the underlying mechanisms governing OS oncogenesis and progression [1,7]. In recent years, the evolution of bioinformatics, particularly single-cell sequencing, has provided enhanced strategies for the exploration and refinement of OS treatments [51,52]. In this study, employing both bulk and single-cell sequencing, we unveiled a substantial association between the immune microenvironment, prognoses, and therapeutic responses in OS patients. Notably, our findings suggest that the differentiation and metabolism of macrophages play a pivotal role in contributing to the chemotherapeutic effects observed in OS. Furthermore, utilizing WGCNA, we identified MRGs and devised an innovative MLMR prognostic model. The resultant integrated nomogram, demonstrating exceptional predictive capabilities, furnishes OS clinicians and patients with more refined prognostic information. Lastly, our drug sensitivity analysis delineated a spectrum of potential therapeutic agents for OS, thereby expanding the therapeutic repertoire available for OS patients.

The intricacies of OS genotypic landscape render the direct and effective elimination of OS cells challenging [7]. This underscores the imperative need to explore novel therapeutic paradigms for OS. OS cells evolve and interact with the stromal cells and immune cells, forming the tumor microenvironment and affecting the progression of tumor, including proliferation, metastasis, vascularization, and drug resistance [53]. Therefore, targeting the stromal and/or immune cells may serve as a promising way for OS treatments. The present study utilized clustering based on metabolism-related pathways to identify the prognosis related pathways and found that immune related pathway were highly associated with the prognoses of OS patients. Subsequently, immune infiltration analysis indicated that the differentiation state of macrophages may be associated with the chemotherapeutic effects of OS patients, and the dominance distribution of the predifferentiated macrophages were likely in connection with poor chemotherapeutic effects. Furthermore, the utilization of single-cell sequencing confirmed our hypothesis, revealing that predifferentiated macrophages predominantly populate the tumor microenvironment in OS cases with suboptimal chemotherapeutic responses. This finding suggests that the activation of macrophages holds promise as a viable strategy for enhancing the therapeutic efficacy of OS treatments. Admittedly, the activation of macrophages was proved as a viable method for OS treatments [18,54,55]. Mifamurtide, which could activate the innate immune system via NOD2, was found to be well-tolerated and effective in OS patients [55,56]. Additionally, the inhibition of the CD47–SIRP $\alpha$  signaling pathway has been tried to serve as a potential method to activate tumor-associated macrophages for OS treatments [57–60]. Previous studies found that macrophages might alter the OS tumor microenvironment to affect the chemotherapeutic effects of OS patients [61,62]. The single-cell sequencing analysis in this study displayed that differentiated macrophages exhibited more immune potential and were the major population in OS patients with better chemotherapeutic effect. Therefore, activation of macrophages may serve as the potential method for OS treatments and/or adjuvant therapies.

Metabolism pattern has been found to involve in the regulation of macrophage plasticity [63,64]. In the present study, to further explore the metabolism discrepancy of macrophages between good- and poor-chemotherapeutic OS, we performed a metabolic analysis and found lipid metabolism related pathways were enriched in macrophages of the poor-chemotherapeutic OS. Additionally, a serious lipid metabolism related molecule, such as CD36, APOE, APOC1, and LIPA were higher expressed in macrophages of the poor-chemotherapeutic OS, which indicate that high lipid metabolism may contribute to the poor immune response of these macrophages. Increasing evidence has confirmed the lipid metabolism plays an important role in macrophage phenotype and function, eventually affecting the occurrence and progression of various diseases [65,66]. Considering the significant role of macrophage in OS and the regulation of lipid metabolism in macrophages plasticity, we tried to construct MLMR prognostic predictors for the clinicians and OS patients, which may contribute to precise diagnosis, treatment optimization, and prognosis assessment. Through univariate and multivariate cox regression analyses, a MLMR risk was constructed and exhibited an excellent prognostic predictive ability in both training and testing cohorts. Subsequently, the functional enrichment analyses and immune infiltration analysis demonstrated that the underlying mechanism of our risk model might attribute to the difference of the immune response. Compared with the high-risk group, the low-risk group distinctly exhibited more immune infiltration and response. However, the MLMR risk model succeeded in a qualitative prognosis while failed to provide more precise prognostic information that may benefit the more specific treatment of OS patients. To address this issue, we established a MLMR nomogram integrating risk score and prognosis related clinical traits to offer the quantitative prognostic information. Considering the integration of the well-known prognostic factors including OS metastasis and primary site, the construction of MLMR nomogram would undoubtedly improve the predictive efficiency of the MLMR prognostic model. Furthermore, the corresponding calibration, timeROC, and timeDCA curve of the nomogram also revealed its high performance

in term of predictive accuracy and clinical usefulness.

Since the application of high-dose methotrexate, vincristine and folic acid as OS adjuvant chemotherapy in the 1870s, the survival rate of patients have been distinctly improved and the multidrug combination chemotherapy has therefore become the basic chemotherapy regimen for OS treatments [67]. The conventional chemotherapy drugs, including doxorubicin, cisplatin, methotrexate, and isocyclophosphamide, have good chemotherapy reactivity in about 70% of patients while fail to reach a satisfactory outcome in patients with relapsing and/or metastatic OS [68]. Furthermore, the increasing chemoresistance has discounted the therapeutic effects of these conventional medications, narrowing the drug selection of OS for the clinicians and impeding the improvement of OS patient's survival rate [55]. Therefore, exploiting OS alternative medication may benefit to break this deadlock. The present study, based on the MLMR risk model, utilized drug sensitivity analysis to identified a serious of OS potential drugs, such as AZD2014, Sapitinib, Buparlisib, Afuresertib, MIRA-1, and BIBR-1532. Most of these drugs exert their impact on certain OS canonical targets and signaling pathways, such as p53, PI3K/AKT/mTOR pathway, and VEGF-VEGFR pathway [7], which were mostly found abnormal alteration during OS occurrence and progression. Notably, p53, PI3K/AKT/mTOR and VEGF-VEGFR involved in the regulation of lipid metabolism in macrophages and play an important role in the occurrence and progression of various diseases including cancers [69–73]. Additionally, previous studies have shown that Lalistat2, a drug inhibiting lysosomal acid lipase, could be used to target TAMs and hence suppressed the progression of various cancers, which highlighted the potential of MLMR drugs to the cancer treatments [74–76]. Collectively, our drug sensitivity analysis may offer more drug selection for the clinicians and OS patients.

Undoubtedly, the study was confronted with several inherent limitations demanding meticulous scrutiny. Primarily, the accuracy of MLMR risk model necessitates rigorous validation through comprehensive assessments against external datasets. This verification process is imperative to establish the robustness and generalizability of our findings. Moreover, the intricate intricacies surrounding the specific role and regulatory mechanisms governing lipid metabolism in macrophages remain inadequately elucidated. Consequently, it becomes imperative to embark upon further experimental endeavors. These additional investigations should delve deeper into the nuanced interactions within the cellular milieu, shedding light on the intricacies of macrophage lipid metabolism. This holistic exploration will not only fortify the credibility of our current findings but also contribute to a more profound understanding of the underlying biological mechanisms at play.

## 5. Conclusion

In summary, our study demonstrated that the important role of macrophages, of which predifferentiated macrophages were associated with the worse therapeutic effects. Further exploration of macrophages metabolism displayed that lipid metabolism related pathways and genes were enriched in these predifferentiated macrophages. Subsequently, the excellent MLMR risk model and nomogram were established to provide the prognostic information, which may contribute to the diagnostic accuracy improvement, treatment optimization, and prognostic assessment.

## Ethics approval and consent to participate

This study did not involve any human samples and was approved by the Ethics Committee of Xiangya Hospital of Central South University.

## Funding Statement

This work was funded by the Provincial Science and Technology Innovation Plan Project of Hunan (2023SK2023), the Provincial Science Foundation of Hunan (No. 2022JJ30075), Special funds for the construction of innovative provinces in Hunan Province (2020RC3058).

## Data availability

The datasets supporting our findings are presented in the article.

## Consent for publication

Not applicable.

## CRedit authorship contribution statement

**Zili Lin:** Writing – review & editing, Writing – original draft, Visualization, Validation, Software, Methodology, Investigation, Data curation, Conceptualization. **Ziyi Wu:** Writing – original draft, Software, Methodology, Investigation, Data curation. **Wei Luo:** Writing – review & editing, Validation, Funding acquisition, Conceptualization.

## Declaration of competing interest

The authors declare that they have no known competing financial interests or personal relationships that could have appeared to

influence the work reported in this paper.

The authors declare the following financial interests/personal relationships which may be considered as potential competing interests: Wei Luo reports financial support was provided by the Provincial Science and Technology Innovation Plan Project of Hunan. Wei Luo reports financial support was provided by the Provincial Science and Technology Innovation Plan Project of Hunan. Wei Luo reports financial support was provided by the Provincial Science and Technology Innovation Plan Project of Hunan. If there are other authors, they declare that they have no known competing financial interests or personal relationships that could have appeared to influence the work reported in this paper.

## Acknowledgments

We thank xiangya hospital for their support of this work.

## Appendix A. Supplementary data

Supplementary data to this article can be found online at <https://doi.org/10.1016/j.heliyon.2024.e26091>.

## References

- [1] J. Ritter, S.S. Bielack, Osteosarcoma. *Annals of oncology : official journal of the European Society for Medical Oncology* 21 (Suppl 7) (2010) vii320–325, <https://doi.org/10.1093/annonc/mdq276>.
- [2] P.S. Meltzer, L.J. Helman, New Horizons in the treatment of osteosarcoma, *N. Engl. J. Med.* 385 (2021) 2066–2076, <https://doi.org/10.1056/NEJMra2103423>.
- [3] M. Kansara, M.W. Teng, M.J. Smyth, D.M. Thomas, Translational biology of osteosarcoma, *Nat. Rev. Cancer* 14 (2014) 722–735, <https://doi.org/10.1038/nrc3838>.
- [4] S.C. Kaste, C.B. Pratt, A.M. Cain, D.J. Jones-Wallace, B.N. Rao, Metastases detected at the time of diagnosis of primary pediatric extremity osteosarcoma at diagnosis: imaging features, *Cancer* 86 (1999) 1602–1608, [https://doi.org/10.1002/\(sici\)1097-0142\(19991015\)86:8<1602::aid-cnrc31>3.0.co;2-r](https://doi.org/10.1002/(sici)1097-0142(19991015)86:8<1602::aid-cnrc31>3.0.co;2-r).
- [5] A. Longhi, et al., Late effects of chemotherapy and radiotherapy in osteosarcoma and Ewing sarcoma patients: the Italian Sarcoma Group Experience (1983–2006), *Cancer* 118 (2012) 5050–5059, <https://doi.org/10.1002/cncr.27493>.
- [6] Y. Jiang, et al., Multi-omics analysis identifies osteosarcoma subtypes with distinct prognosis indicating stratified treatment, *Nat. Commun.* 13 (2022) 7207, <https://doi.org/10.1038/s41467-022-34689-5>.
- [7] J. Gill, R. Gorlick, Advancing therapy for osteosarcoma, *Nat. Rev. Clin. Oncol.* 18 (2021) 609–624, <https://doi.org/10.1038/s41571-021-00519-8>.
- [8] S. Zou, et al., Targeting STAT3 in cancer immunotherapy, *Mol. Cancer* 19 (2020) 145, <https://doi.org/10.1186/s12943-020-01258-7>.
- [9] G. Kroemer, L. Galluzzi, O. Kepp, L. Zitvogel, Immunogenic cell death in cancer therapy, *Annu. Rev. Immunol.* 31 (2013) 51–72, <https://doi.org/10.1146/annurev-immunol-032712-100008>.
- [10] M.D. Vesely, M.H. Kershaw, R.D. Schreiber, M.J. Smyth, Natural innate and adaptive immunity to cancer, *Annu. Rev. Immunol.* 29 (2011) 235–271, <https://doi.org/10.1146/annurev-immunol-031210-101324>.
- [11] L. Labanieh, R.G. Majzner, C.L. Mackall, Programming CAR-T cells to kill cancer, *Nat. Biomed. Eng.* 2 (2018) 377–391, <https://doi.org/10.1038/s41551-018-0235-9>.
- [12] P.K. Bommareddy, M. Shettigar, H.L. Kaufman, Integrating oncolytic viruses in combination cancer immunotherapy, *Nat. Rev. Immunol.* 18 (2018) 498–513, <https://doi.org/10.1038/s41577-018-0014-6>.
- [13] L. Maiorino, J. Daßler-Plenker, L. Sun, M. Egeblad, Innate immunity and cancer Pathophysiology, *Annual review of pathology* 17 (2022) 425–457, <https://doi.org/10.1146/annurev-pathmechdis-032221-115501>.
- [14] A. van Weverwijk, K.E. de Visser, Mechanisms driving the immunoregulatory function of cancer cells, *Nat. Rev. Cancer* 23 (2023) 193–215, <https://doi.org/10.1038/s41568-022-00544-4>.
- [15] S. Wang, et al., Metabolic reprogramming of macrophages during infections and cancer, *Cancer letters* 452 (2019) 14–22, <https://doi.org/10.1016/j.canlet.2019.03.015>.
- [16] C. Wei, et al., Crosstalk between cancer cells and tumor associated macrophages is required for mesenchymal circulating tumor cell-mediated colorectal cancer metastasis, *Mol. Cancer* 18 (2019) 64, <https://doi.org/10.1186/s12943-019-0976-4>.
- [17] B.Z. Qian, J.W. Pollard, Macrophage diversity enhances tumor progression and metastasis, *Cell* 141 (2010) 39–51, <https://doi.org/10.1016/j.cell.2010.03.014>.
- [18] E.P. Buddingh, et al., Tumor-infiltrating macrophages are associated with metastasis suppression in high-grade osteosarcoma: a rationale for treatment with macrophage activating agents, *Clin. Cancer Res. : an official journal of the American Association for Cancer Research* 17 (2011) 2110–2119, <https://doi.org/10.1158/1078-0432.Ccr-10-2047>.
- [19] Y. Han, et al., Tumor-associated macrophages promote lung metastasis and induce epithelial-mesenchymal transition in osteosarcoma by activating the COX-2/STAT3 axis, *Cancer letters* 440–441 (2019) 116–125, <https://doi.org/10.1016/j.canlet.2018.10.011>.
- [20] C. Dumars, et al., Dysregulation of macrophage polarization is associated with the metastatic process in osteosarcoma, *Oncotarget* 7 (2016) 78343–78354, <https://doi.org/10.18632/oncotarget.13055>.
- [21] A.I. Ségaliny, et al., Interleukin-34 promotes tumor progression and metastatic process in osteosarcoma through induction of angiogenesis and macrophage recruitment, *Int. J. Cancer* 137 (2015) 73–85, <https://doi.org/10.1002/ijc.29376>.
- [22] Q. Zhou, et al., All-trans Retinoic acid Prevents osteosarcoma metastasis by inhibiting M2 polarization of tumor-associated macrophages, *Cancer Immunol. Res.* 5 (2017) 547–559, <https://doi.org/10.1158/2326-6066.Cir-16-0259>.
- [23] S. Wang, et al., Metabolic reprogramming of macrophages during infections and cancer, *Cancer letters* 452 (2019) 14–22, <https://doi.org/10.1016/j.canlet.2019.03.015>.
- [24] K. Mehla, P.K. Singh, Metabolic regulation of macrophage polarization in cancer, *Trends in cancer* 5 (2019) 822–834, <https://doi.org/10.1016/j.trecan.2019.10.007>.
- [25] Y. Cao, Adipocyte and lipid metabolism in cancer drug resistance, *The Journal of clinical investigation* 129 (2019) 3006–3017, <https://doi.org/10.1172/jci127201>.
- [26] X. Bian, et al., Lipid metabolism and cancer, *The Journal of experimental medicine* 218 (2021), <https://doi.org/10.1084/jem.20201606>.
- [27] L.A. Broadfield, A.A. Pane, A. Talebi, J.V. Swinnen, S.M. Fendt, Lipid metabolism in cancer: new perspectives and emerging mechanisms, *Dev. Cell* 56 (2021) 1363–1393, <https://doi.org/10.1016/j.devcel.2021.04.013>.
- [28] S.A. Lim, W. Su, N.M. Chapman, H. Chi, Lipid metabolism in T cell signaling and function, *Nat. Chem. Biol.* 18 (2022) 470–481, <https://doi.org/10.1038/s41589-022-01017-3>.

- [29] A. Bleve, B. Durante, A. Sica, F.M. Consonni, Lipid metabolism and cancer immunotherapy: immunosuppressive Myeloid cells at the Crossroad, *Int. J. Mol. Sci.* 21 (2020), <https://doi.org/10.3390/ijms21165845>.
- [30] P. Su, et al., Enhanced lipid accumulation and metabolism are required for the differentiation and activation of tumor-associated macrophages, *Cancer Res.* 80 (2020) 1438–1450, <https://doi.org/10.1158/0008-5472.Can-19-2994>.
- [31] J. Yan, T. Horng, Lipid metabolism in regulation of macrophage functions, *Trends Cell Biol.* 30 (2020) 979–989, <https://doi.org/10.1016/j.tcb.2020.09.006>.
- [32] A. Batista-Gonzalez, R. Vidal, A. Criollo, L.J. Carreño, New insights on the role of lipid metabolism in the metabolic reprogramming of macrophages, *Front. Immunol.* 10 (2019) 2993, <https://doi.org/10.3389/fimmu.2019.02993>.
- [33] S. Saha, I.N. Shalova, S.K. Biswas, Metabolic regulation of macrophage phenotype and function, *Immunol. Rev.* 280 (2017) 102–111, <https://doi.org/10.1111/immr.12603>.
- [34] E. Vassiliou, R. Farias-Pereira, Impact of lipid metabolism on macrophage polarization: Implications for inflammation and tumor immunity, *Int. J. Mol. Sci.* 24 (2023), <https://doi.org/10.3390/ijms241512032>.
- [35] J. Taminau, et al., Unlocking the potential of publicly available microarray data using inSilicoDb and inSilicoMerging R/Bioconductor packages, *BMC Bioinf.* 13 (2012) 335, <https://doi.org/10.1186/1471-2105-13-335>.
- [36] J.T. Leek, W.E. Johnson, H.S. Parker, A.E. Jaffe, J.D. Storey, The sva package for removing batch effects and other unwanted variation in high-throughput experiments, *Bioinformatics* 28 (2012) 882–883, <https://doi.org/10.1093/bioinformatics/bts034>.
- [37] A. Gribov, et al., SEURAT: visual analytics for the integrated analysis of microarray data, *BMC Med. Genom.* 3 (2010) 21, <https://doi.org/10.1186/1755-8794-3-21>.
- [38] I. Korsunsky, et al., Fast, sensitive and accurate integration of single-cell data with Harmony, *Nat. Methods* 16 (2019) 1289–1296, <https://doi.org/10.1038/s41592-019-0619-0>.
- [39] M.D. Wilkerson, D.N. Hayes, ConsensusClusterPlus: a class discovery tool with confidence assessments and item tracking, *Bioinformatics* 26 (2010) 1572–1573, <https://doi.org/10.1093/bioinformatics/btq170>.
- [40] G. Nyamundanda, P. Poudel, Y. Patil, A. Sadanandam, A novel statistical method to Diagnose, quantify and Correct batch effects in genomic studies, *Sci. Rep.* 7 (2017) 10849, <https://doi.org/10.1038/s41598-017-11110-6>.
- [41] G. Yu, L.G. Wang, Y. Han, Q.Y. He, clusterProfiler: an R package for comparing biological themes among gene clusters, *OMICS A J. Integr. Biol.* 16 (2012) 284–287, <https://doi.org/10.1089/omi.2011.0118>.
- [42] K. Yoshihara, et al., Inferring tumour purity and stromal and immune cell admixture from expression data, *Nat. Commun.* 4 (2013) 2612, <https://doi.org/10.1038/ncomms3612>.
- [43] A.M. Newman, et al., Robust enumeration of cell subsets from tissue expression profiles, *Nat. Methods* 12 (2015) 453–457, <https://doi.org/10.1038/nmeth.3337>.
- [44] H. Lu, et al., CommPath: an R package for inference and analysis of pathway-mediated cell-cell communication chain from single-cell transcriptomics, *Comput. Struct. Biotechnol. J.* 20 (2022) 5978–5983, <https://doi.org/10.1016/j.csbj.2022.10.028>.
- [45] C. Chen, et al., Comprehensive single-cell transcriptomic and proteomic analysis reveals NK cell exhaustion and unique tumor cell evolutionary trajectory in non-keratinizing nasopharyngeal carcinoma, *J. Transl. Med.* 21 (2023) 278, <https://doi.org/10.1186/s12967-023-04112-8>.
- [46] Y. Wu, et al., Spatiotemporal immune landscape of colorectal cancer Liver metastasis at single-cell level, *Cancer Discov.* 12 (2022) 134–153, <https://doi.org/10.1158/2159-8290.Cd-21-0316>.
- [47] P. Langfelder, S. Horvath, WGCNA: an R package for weighted correlation network analysis, *BMC Bioinf.* 9 (2008) 559, <https://doi.org/10.1186/1471-2105-9-559>.
- [48] M.E. Ritchie, et al., Limma powers differential expression analyses for RNA-sequencing and microarray studies, *Nucleic acids research* 43 (2015) e47, <https://doi.org/10.1093/nar/gkv007>.
- [49] M.J. Whitehead, G.A. McCanney, H.J. Willison, S.C. Barnett, MyelinJ: an ImageJ macro for high throughput analysis of myelinating cultures, *Bioinformatics* 35 (2019) 4528–4530, <https://doi.org/10.1093/bioinformatics/btz403>.
- [50] D. Maeser, R.F. Gruener, R.S. Huang, oncoPredict: an R package for predicting in vivo or cancer patient drug response and biomarkers from cell line screening data, *Briefings Bioinf.* 22 (2021), <https://doi.org/10.1093/bib/bbab260>.
- [51] Y. Zhou, et al., Single-cell RNA landscape of intratumoral heterogeneity and immunosuppressive microenvironment in advanced osteosarcoma, *Nat. Commun.* 11 (2020) 6322, <https://doi.org/10.1038/s41467-020-20059-6>.
- [52] A.R. Cillo, et al., Ewing sarcoma and osteosarcoma have distinct immune Signatures and intercellular communication networks, *Clin. Cancer Res. : an official journal of the American Association for Cancer Research* 28 (2022) 4968–4982, <https://doi.org/10.1158/1078-0432.Ccr-22-1471>.
- [53] C.C. Wu, et al., Immuno-genomic landscape of osteosarcoma, *Nat. Commun.* 11 (2020) 1008, <https://doi.org/10.1038/s41467-020-14646-w>.
- [54] A. Nardin, M.L. Lefebvre, K. Labroquère, O. Faure, J.P. Abastado, Liposomal muramyl tripeptide phosphatidylethanolamine: targeting and activating macrophages for adjuvant treatment of osteosarcoma, *Curr. Cancer Drug Targets* 6 (2006) 123–133, <https://doi.org/10.2174/156800906776056473>.
- [55] P.M. Anderson, et al., Mifamurtide in metastatic and recurrent osteosarcoma: a patient access study with pharmacokinetic, pharmacodynamic, and safety assessments, *Pediatr. Blood Cancer* 61 (2014) 238–244, <https://doi.org/10.1002/pbc.24686>.
- [56] N. Gisch, B. Buske, H. Heine, B. Lindner, U. Zähringer, Synthesis of biotinylated muramyl tripeptides with NOD2-stimulating activity, *Bioorg. Med. Chem. Lett* 21 (2011) 3362–3366, <https://doi.org/10.1016/j.bmcl.2011.04.005>.
- [57] J.F. Xu, et al., CD47 blockade inhibits tumor progression human osteosarcoma in xenograft models, *Oncotarget* 6 (2015) 23662–23670, <https://doi.org/10.18632/oncotarget.4282>.
- [58] J. Theruvath, et al., Anti-GD2 synergizes with CD47 blockade to mediate tumor eradication, *Nature medicine* 28 (2022) 333–344, <https://doi.org/10.1038/s41591-021-01625-x>.
- [59] Anti-GD2 and anti-CD47 are Synergistic and promote tumor eradication, *Cancer Discov.* 12 (2022) Of8, <https://doi.org/10.1158/2159-8290.Cd-rw2022-011>.
- [60] S. Fang, et al., Anti-CD47 antibody eliminates bone tumors in rats, *Saudi J. Biol. Sci.* 26 (2019) 2074–2078, <https://doi.org/10.1016/j.sjbs.2019.09.011>.
- [61] X. Liang, et al., Macrophages reduce the sensitivity of osteosarcoma to neoadjuvant chemotherapy drugs by secreting Interleukin-1 beta, *Cancer letters* 480 (2020) 4–14, <https://doi.org/10.1016/j.canlet.2020.03.019>.
- [62] E.S. Kleinerman, J.S. Snyder, N. Jaffe, Influence of chemotherapy administration on monocyte activation by liposomal muramyl tripeptide phosphatidylethanolamine in children with osteosarcoma, *J. Clin. Oncol. : official journal of the American Society of Clinical Oncology* 9 (1991) 259–267, <https://doi.org/10.1200/jco.1991.9.2.259>.
- [63] M. Locati, G. Curtale, A. Mantovani, Diversity, mechanisms, and significance of macrophage plasticity, *Annual review of pathology* 15 (2020) 123–147, <https://doi.org/10.1146/annurev-pathmechdis-012418-012718>.
- [64] I. Vitale, G. Manic, L.M. Coussens, G. Kroemer, L. Galluzzi, Macrophages and metabolism in the tumor microenvironment, *Cell Metabol.* 30 (2019) 36–50, <https://doi.org/10.1016/j.cmet.2019.06.001>.
- [65] A. Remmerie, C.L. Scott, Macrophages and lipid metabolism, *Cell. Immunol.* 330 (2018) 27–42, <https://doi.org/10.1016/j.cellimm.2018.01.020>.
- [66] J. Yan, T. Horng, Lipid metabolism in regulation of macrophage functions, *Trends Cell Biol.* 30 (2020) 979–989, <https://doi.org/10.1016/j.tcb.2020.09.006>.
- [67] N. Jaffe, E. Frei 3rd, D. Traggis, Y. Bishop, Adjuvant methotrexate and citrovorum-factor treatment of osteogenic sarcoma, *N. Engl. J. Med.* 291 (1974) 994–997, <https://doi.org/10.1056/nejm197411072911902>.
- [68] K.A. Janeway, H.E. Grier, Sequelae of osteosarcoma medical therapy: a review of rare acute toxicities and late effects, *Lancet Oncol.* 11 (2010) 670–678, [https://doi.org/10.1016/s1470-2045\(10\)70062-0](https://doi.org/10.1016/s1470-2045(10)70062-0).
- [69] J. Miao, et al., Paeonol enhances macrophage phagocytic function by modulating lipid metabolism through the P53-TREM2 axis, *Front. Pharmacol.* 14 (2023) 1214756, <https://doi.org/10.3389/fphar.2023.1214756>.
- [70] Y. Huang, et al., Inflammasome activation and Pyroptosis via a lipid-regulated SIRT1-p53-ASC Axis in macrophages from Male mice and humans, *Endocrinology* 163 (2022), <https://doi.org/10.1210/endo/bqac014>.

- [71] L.L. Chen, W.J. Wang, p53 regulates lipid metabolism in cancer, *Int. J. Biol. Macromol.* 192 (2021) 45–54, <https://doi.org/10.1016/j.ijbiomac.2021.09.188>.
- [72] J.Y. Kou, et al., Berberine-sonodynamic therapy induces autophagy and lipid unloading in macrophage, *Cell Death Dis.* 8 (2017) e2558, <https://doi.org/10.1038/cddis.2016.354>.
- [73] B. Liu, et al., Scoparone improves hepatic inflammation and autophagy in mice with nonalcoholic steatohepatitis by regulating the ROS/P38/Nrf2 axis and PI3K/AKT/mTOR pathway in macrophages, *Biomedicine & pharmacotherapy = Biomedecine & pharmacotherapie* 125 (2020) 109895, <https://doi.org/10.1016/j.biopha.2020.109895>.
- [74] S. Schlager, et al., Lysosomal lipid hydrolysis provides substrates for lipid mediator synthesis in murine macrophages, *Oncotarget* 8 (2017) 40037–40051, <https://doi.org/10.18632/oncotarget.16673>.
- [75] I. Bradić, et al., Off-target effects of the lysosomal acid lipase inhibitors Lalistat-1 and Lalistat-2 on neutral lipid hydrolases, *Mol. Metabol.* 61 (2022) 101510, <https://doi.org/10.1016/j.molmet.2022.101510>.
- [76] P.K. Panda, et al., Deacetylation of LAMP1 drives lipophagy-dependent generation of free fatty acids by Abrus agglutinin to promote senescence in prostate cancer, *J. Cell. Physiol.* 235 (2020) 2776–2791, <https://doi.org/10.1002/jcp.29182>.